

# Some experimental results on thin polypropylene films loaded with finely-dispersed copper

S. A. Y. AL-ISMAIL, C. A. HOGARTH  
*Department of Physics, Brunel University, Middlesex, UK*

Experiments have shown that small additions of copper to polymer film where both components are deposited from the vapour phase, and the copper content is in the range of 0.1 to 1.0% by weight, can have a profound effect on the electrical conductivity of the polymer films and a special system of boats for the evaporation sources was devised to enable films of controlled composition to be produced. Structural studies using the electron microscope and X-ray photoelectron spectroscopy show that the copper is finely dispersed within the polypropylene matrix with grain size of the order of  $10\ \mu\text{m}$  diameter and that some of the copper has been converted to copper oxide, but the composite film retains its overall amorphous structure. Electrical measurements on polypropylene samples loaded with 0.15% copper by weight show (a) for MIM sandwich structures with typical dielectric thickness of 300 nm, ohmic  $V-I$  characteristics up to approximately  $10^6\ \text{V cm}^{-1}$  and a space-charge-limited characteristic beyond that, and (b) for planar structures with typical effective inter-electrode separation of 0.05 cm, ohmic  $V-I$  characteristics up to approximately  $2 \times 10^3\ \text{V cm}^{-1}$  and beyond that a high-field conduction of the Poole-Frenkel type. For both types of samples a trapping centre at 0.33 to 0.34 eV is estimated. The planar structure shows considerable photosensitivity.

## 1. Introduction

There is a variety of techniques which may be invoked in the development of polymeric materials of controllable electrical resistivity and with photosensitivity. One major line of research involves the preparation and study of the polyacetylenes. Another line, which we have followed, involves the preparation of thin film polymer samples loaded with metal in finely dispersed form as originally proposed by Boonthanom and White [1]. We have studied a variety of evaporated polymer films and the earlier results have been reviewed by Hogarth and Iqbal [2]. Unlike Boonthanom and White we have had the advantage of readily available X-ray photoelectron spectroscopy (XPS) analytical techniques and have been able to monitor rapidly the metal content of the films. The advantage of the polymer-metal system is simply that the metal can be dispersed in very fine particulate form in the polymer and the content can be carefully controlled if a co-evaporation technique involving two independent sources is employed. The metal is generally more finely dispersed than for films containing metal particles added by the normal polymer chemical techniques before the films are extruded or blown, and would therefore be expected to interact on a larger scale with its polymer host since the total surface area of a given metal admixture would be greater. We have studied a variety of thin film polymer systems and in this presentation we are giving examples of films of polypropylene loaded with a copper content of 0.15 wt %.

## 2. Experimental techniques

A novel source for polymer evaporation has been devised and built from pyrophyllite with a cover in the form of a stainless steel pepper pot with a cone to one side to direct copper vapour into a mixing chamber. This arrangement makes up for the speed with which metal may be evaporated and gives a good control over the amount of metal evaporated along with the polymer. The copper is evaporated from a molybdenum strip source. The whole system is subject to manual control of heater currents, the deposition rate being recorded by quartz crystal monitors. The source temperatures were recorded using chromel-alumel thermocouples. The polypropylene-copper films were deposited on cleaned Corning glass 7059 substrates in a modified Edwards 19E7 coating unit, the substrate temperature being  $\approx 80^\circ\text{C}$ . In spite of fairly fast pumps the pressure in the system rose to nearly  $10^{-4}$  torr during the co-evaporation mainly because of the light fragments produced during the thermal degradation of the polypropylene. The evaporation rates were 1.3 to  $2.6\ \text{nm min}^{-1}$  for the polymer and 5 to  $10\ \text{nm min}^{-1}$  for the copper. Two types of sample were made (a) in normal metal-insulator-metal (MIM) sandwich form with dielectric dimensions  $0.3 \times 0.5 \times (4 \times 10^{-6})\ \text{cm}^3$  and (b) in planar form with an effective inter-electrode spacing of 0.5 mm.

D.c. electrical measurements were made in a subsidiary vacuum system ( $10^{-5}$  torr) and by heating or by liquid nitrogen cooling the range  $100^\circ\text{C}$  to  $-60^\circ\text{C}$

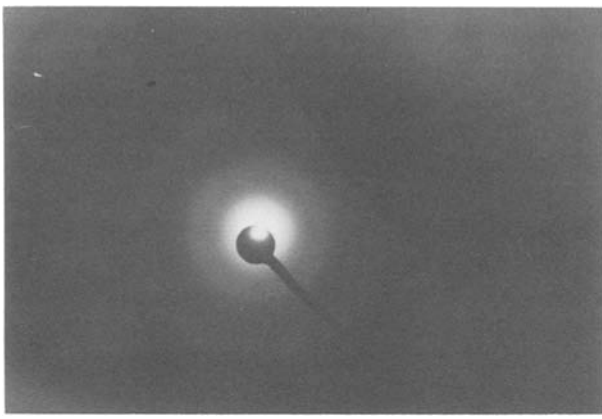


Figure 1 Electron diffraction pattern of an evaporated film of polypropylene containing finely-dispersed copper.

could readily be covered, the sample temperatures being recorded by thermocouples.

Structural measurements were made using well-established techniques of X-ray diffraction, XPS and the electron probe microanalyser to determine the main chemical species present in the composite films.

### 3. Results

#### 3.1. Structural examination

Electron diffraction examination of samples shows a pattern of the very diffuse rings or haloes typical of amorphous or very finely-grained material as shown in Fig. 1. The electron micrograph shown in Fig. 2 indicates the fineness of the dispersion of the copper particles, and the copper-line of the electron probe microanalyser confirms that in general the dark patches represent the grains of copper. A typical grain dimension is seen to be of the order of  $10 \mu\text{m}$ .

The XPS analysis of a film is given in Fig. 3 and shows the presence in the film of high concentrations of copper and oxygen as well as a much smaller peak due to carbon. The oxygen probably arises from the higher pressures during the evaporation and from the original copper.

#### 3.2. Electrical measurements

Figs 4a and b show typical  $V_b - I_c$  plots for (a) the sandwich and (b) the planar specimens. Above

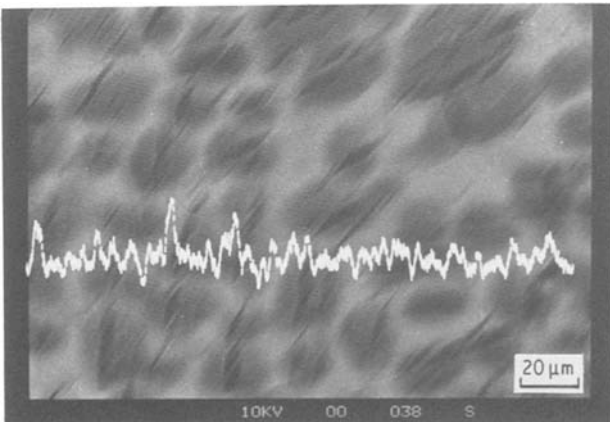


Figure 2 Electron micrograph of a polypropylene-copper film together with a microprobe trace with the line tuned to copper.

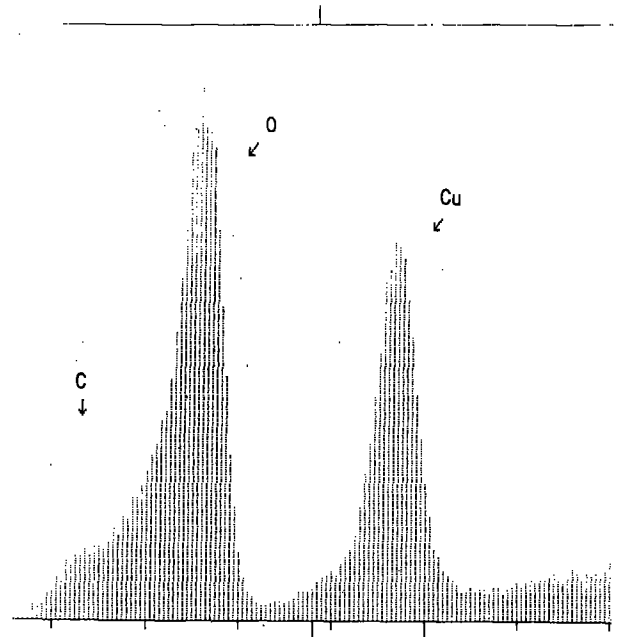


Figure 3 XPS data for an evaporated polypropylene-copper thin film.

$V_b = 50 \text{ V}$  the current shows a square-law dependence on voltage indicating a space-charge-limited (SCL) conduction process. SCL currents for samples containing a single trapping level are described by the equation for the current density [3]

$$J_s \approx \frac{10^{-13} V_b \mu \theta \epsilon}{d^3} \quad (1)$$

where  $V_b$  is the bias voltage,  $\mu$  is the carrier mobility,  $\epsilon$  is the relative dielectric constant,  $d$  is the insulator thickness and  $\theta$  is a function of the ratio of free charge

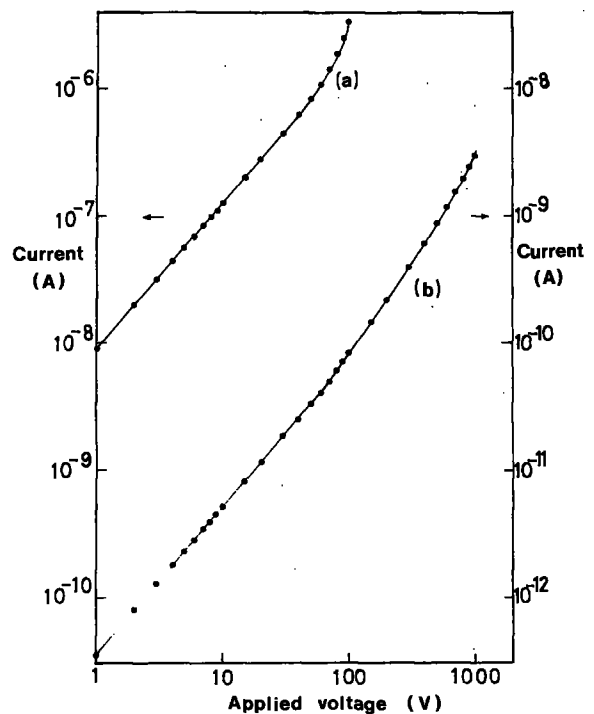


Figure 4 Current as a function of inverse temperature for a metal-polypropylene (copper)-metal sandwich assembly. (Dielectric thickness  $300 \text{ nm}$ ; area  $0.15 \text{ cm}^2$ ;  $V_b = 50 \text{ V}$ ; slope  $-1695 \text{ K}$ ;  $E_t = 0.34 \text{ eV}$ .)

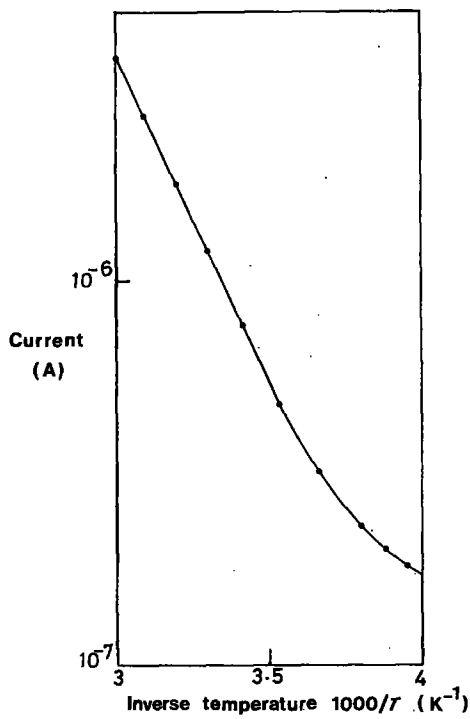


Figure 5 Voltage-current characteristics for metal-polypropylene (copper)-metal assemblies in (a) sandwich and (b) planar configurations. (Dielectric thickness in (a) is 300 nm and effective electrode spacing in (b) is 0.5 mm.)

to trapped charge in the form

$$\theta = \frac{N_c}{N_t} \exp(-E_t/kT) \quad (2)$$

$N_c$  is the density of states in the conduction band,  $N_t$  is the density of trapping states and  $E_t$  is the activation energy of the electron traps. The cross-over voltage  $V_{tr}$

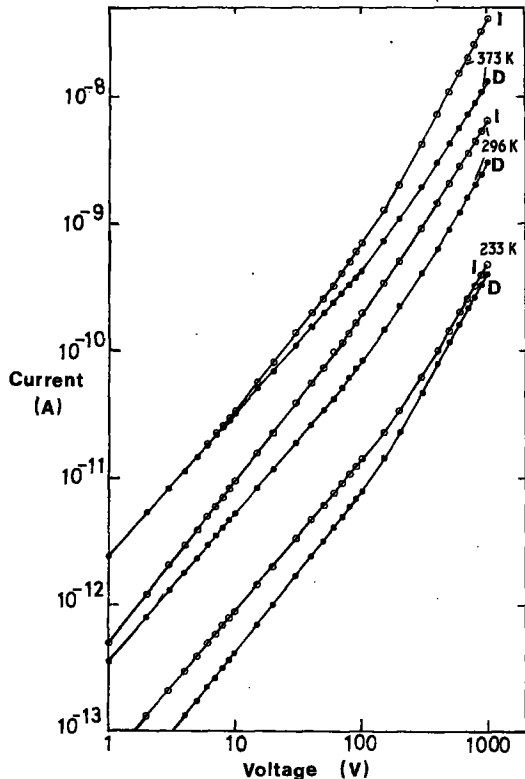


Figure 6 Voltage-current characteristics for a metal-polypropylene (copper)-metal planar sample showing the effect of illumination. (I is illuminated; D is dark.)

TABLE I Voltage-current characteristics of planar samples

Temperature (K)	Slope ( $V^{-1/2}$ )	$\beta_{exp}$ ( $10^{-5} \text{ eV V}^{-1/2} \text{ cm}^{1/2}$ )	$\epsilon_R$ (calculated)
<i>In the dark</i>			
373	0.021	34.7	4.8
296	0.025	32.9	5.3
233	0.029	30.0	6.4
<i>Illuminated</i>			
373	0.026	42.3	3.2
296	0.025	32.9	5.3
233	0.025	32.9	5.3

from the ohmic to the square-law region is given by

$$V_{tr} \approx \frac{10^{13} en_0 d^2}{\epsilon \theta} \quad (3)$$

where  $n_0$  is the free-electron concentration and  $e$  is the electronic charge. On increasing the value of  $V_b$  there will be a point at which the quasi-Fermi level crosses  $E_t$  and this voltage is known as the trap-filled limit (TFL) voltage and is given by [4]

$$V_{TFL} \approx \frac{5.7 \times 10^{12} e N_t d^2}{\epsilon} \quad (4)$$

At this voltage the shallow traps are assumed to be filled and a sharp increase in  $I_c$  will be expected by an amount  $\theta^{-1}$ .

The activation energy involved in the conduction mechanism at 50 V is estimated from Fig. 4 as 0.34 eV. The values of  $n_0$ ,  $N_t$ ,  $\theta$  and  $\mu$  can be estimated from Figs 4 and 5 using Equations 1 to 4. If  $N_c$  is  $1.0 \times 10^{20} \text{ cm}^{-3}$ ,  $\epsilon_R = 5.3$  (measured independently),  $V_b = 50 \text{ V}$ ,  $V_{TFL} = 100 \text{ V}$ , then calculation yields the following:  $d(300 \text{ nm})$ ;  $T(300 \text{ K})$ ;  $N_t(6.5 \times 10^{17} \text{ cm}^{-3})$ ;  $\theta(1.9 \times 10^{-4})$ ;  $n_0(9.9 \times 10^{13} \text{ cm}^{-3})$ ;  $\mu(4.6 \times 10^{-8} \text{ cm}^2 \text{ V}^{-1} \text{ S}^{-1})$ . The ohmic (low-field) region is believed to be controlled by electron hopping. In the presence of deep traps their energy should be below the Fermi energy and the ohmic region would be continued up to the TFL since for example doubling the concentration of thermally-ionized free charge carriers at the TFL will cause the Fermi level to sweep upward from its original level by  $\Delta E_F = kT \ln 2$  i.e. by  $0.7 kT$  and such an increase will fill the deep traps. For shallow traps, their energies lie above the Fermi level and the ohmic region is followed by a square-law region which is caused by the quasi-Fermi level sweeping across the trapping level. The interfaces between the crystalline copper grains and the polypropylene matrix contribute to the trapping of carriers in the sandwich structure.

The planar samples are more difficult to analyse but are of greater significance since they show a marked sensitivity to white light. Fig. 6 shows the  $V_b-I_c$  characteristics for such a sample at three temperatures both illuminated and in the dark and Fig. 7 shows the same data plotted in accordance with normal high-field theory to establish the Poole-Frenkel effect. The results are given in Table I. The field-lowering coefficient  $\beta_{exp}$  increases generally with both temperature and illumination and the variation of the derived value of  $\epsilon_R$  with temperature and illumination is broadly as expected for a partly lossy dielectric.

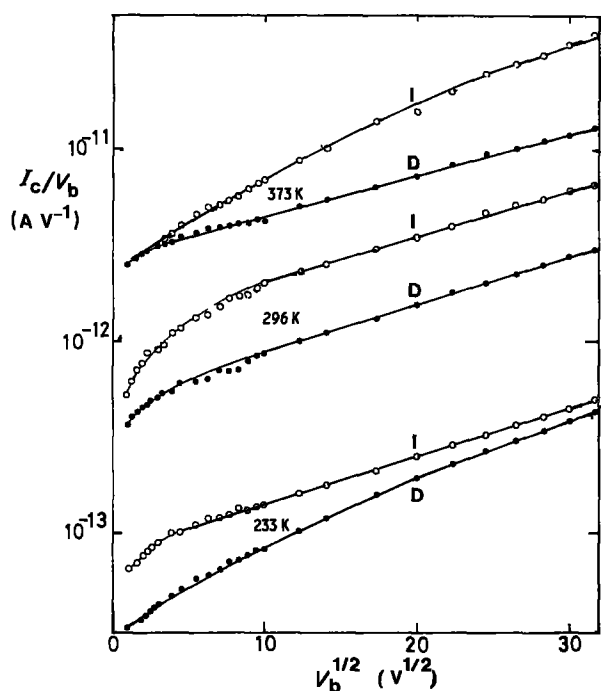


Figure 7 The curves of Fig. 6 replotted to show the form of the high-field regions.

The temperature dependence of current in these devices is exemplified in Fig. 8. In the dark the transitions between conduction mechanisms occur at 35 and 77°C and when illuminated at 10 and 80°C. The calculated activation energies are listed in Table II along with estimates of the carrier mobilities. There is an uncertainty in the values, particularly at the higher temperatures because of difficulties in defining precisely the active sample area when using a planar structure. However our estimates are consistent with an activated mobility going to higher values at higher temperatures and when illuminated.

#### 4. Conclusions

The electrical measurements on samples in the form of MIM sandwiches are more easily analysed than the planar samples. In the sandwich structure the controlling mechanism beyond 50 V applied is space-charge-limited conduction with a very low carrier mobility as stated. For both structures we find the same level of approximately 0.33 to 0.34 eV for the

TABLE II Calculated activation energies in planar samples

	Activation energy $\Delta E$ (eV)	Estimated mobility ( $\text{cm}^2 \text{V}^{-1} \text{s}^{-1}$ )
<i>In the dark</i>		
$T < 35^\circ \text{C}$	0.06	$2 \times 10^{-9}$
$35^\circ \text{C} < T < 77^\circ \text{C}$	0.33	$9 \times 10^{-5}$
$T > 77^\circ \text{C}$	0.52	2.9
<i>Illuminated</i>		
$T < 10^\circ \text{C}$	0.04	$2 \times 10^{-9}$
$10^\circ \text{C} < T < 80^\circ \text{C}$	0.34	$2 \times 10^{-4}$
$T > 80^\circ \text{C}$	0.50	3.3

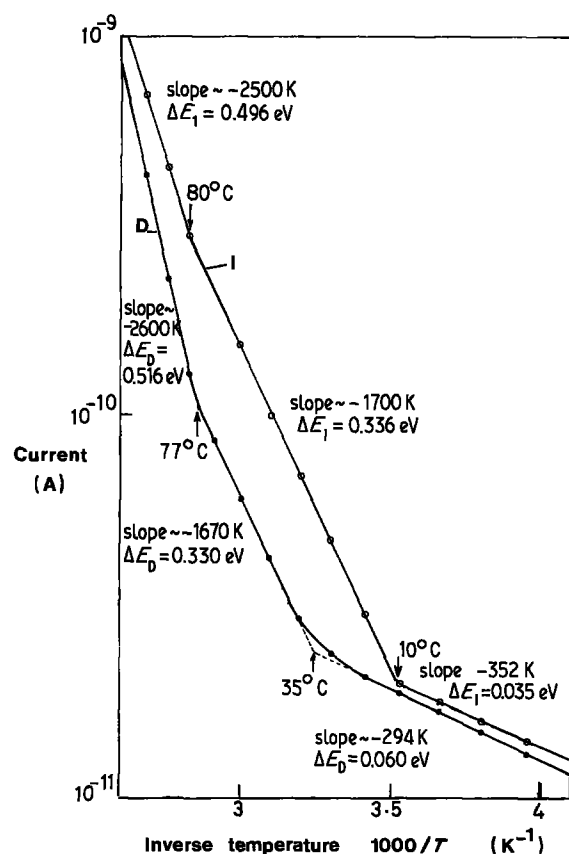


Figure 8 Current as a function of inverse temperature for a planar sample. ( $V_b = 100 \text{ V}$ ; effective electrode separation 0.5 mm.)

trapping centres from which electrons may be excited, as would be expected since we are dealing with the same insulating material.

The dielectric constant generally decreased with increasing temperature and illumination. At intermediate temperatures it seems that photon-electron interactions are stronger than electron-phonon interactions. The photo-current at low temperatures is strongly influenced by traps.

The planar devices show a significant sensitivity to light and may be capable of developing into useful practical components.

#### Acknowledgement

We are pleased to acknowledge the financial support from the Science and Engineering Research Council which funded this investigation.

#### References

1. N. BOONTHANOM and M. WHITE, *Thin Solid Films* **24** (1974) 295.
2. C. A. HOGARTH and T. IQBAL, *Phys. Status Solidi (a)* **65** (1981) 11.
3. A. ROSE, *Phys. Rev.* **97** (1955) 1538.
4. M. A. LAMPERT, *Reports Progr. Phys.* **27** (1964) 329.

Received 26 February  
and accepted 22 May 1986